
¹¹C-NS14492 as a Novel PET Radioligand for Imaging Cerebral α_7 Nicotinic Acetylcholine Receptors: In Vivo Evaluation and Drug Occupancy Measurements

Anders Ettrup¹, Jens D. Mikkelsen^{1,2}, Szabolcs Lehel³, Jacob Madsen³, Elsebet Ø. Nielsen², Mikael Palner¹, Daniel B. Timmermann², Dan Peters², and Gitte M. Knudsen¹

¹Neurobiology Research Unit, Copenhagen University Hospital, Rigshospitalet, Copenhagen, Denmark; ²NeuroSearch A/S, Ballerup, Denmark; and ³PET and Cyclotron Unit, Copenhagen University Hospital, Rigshospitalet, Copenhagen, Denmark

Small-molecule α_7 nicotinic acetylcholine receptor (α_7 nAChR) agonists are currently validated for use as treatment for cognitive disturbances in schizophrenia and in Alzheimer disease. A suitable radiolabeled α_7 nAChR PET tracer would be important for in vivo quantification of α_7 nAChR binding in humans and to measure α_7 nAChR occupancy of α_7 nAChR drug candidates. Here, we present the radiosynthesis and in vivo evaluation of ¹¹C-NS14492 as a selective α_7 nAChR PET radioligand. **Methods:** The high-affinity α_7 nAChR-selective partial agonist NS14492 was radiolabeled by methylation of its desmethyl precursor using ¹¹C-methyl triflate. Female Danish Landrace pigs were studied at baseline and after intravenous administration of blocking doses of either the α_7 nAChR partial agonist SSR180711 or the unlabeled NS14492. ¹¹C-NS14492 was given as an intravenous bolus injection, and the pigs were scanned for 90 min both at baseline and in the blocked conditions. Arterial blood was collected during the scanning, plasma was counted, and parent compound fraction was determined with radio-high-performance liquid chromatography. PET data were quantified with a graphical analysis with arterial input; ¹¹C-NS14492 regional distribution volumes were calculated, and α_7 nAChR occupancy was determined using an occupancy plot. **Results:** ¹¹C-NS14492 had a high uptake in the pig brain, with the highest binding in the cerebral cortex and thalamus in accordance with α_7 nAChR distribution. Pretreatment with NS14492 and SSR180711 consistently decreased distribution volumes of ¹¹C-NS14492 in all examined regions, in a dose-dependent manner, supporting the finding that the radioligand binds selectively to α_7 nAChR in vivo. **Conclusion:** We report here that ¹¹C-NS14492 is the first, to our knowledge, PET radioligand for α_7 nAChR showing a dose-dependent decline in cerebral binding after receptor blockade. This compound is considered a promising PET tracer for in vivo measurements of α_7 nAChR binding in the human brain.

Key Words: positron emission tomography; novel tracer; porcine; nicotinic acetylcholine receptors; occupancy plot

J Nucl Med 2011; 52:1449–1456

DOI: 10.2967/jnumed.111.088815

Cerebral α_7 nicotinic acetylcholine receptors (α_7 nAChRs) are currently being investigated as a potential therapeutic target for cognitive disturbances in schizophrenia and Alzheimer disease based on data from small open clinical studies (1). Further evidence for such effects has over the last decade been generated in animal models showing that systemic administration of small-molecule α_7 nAChR partial agonists produce effects on several domains of cognition (2). Access to a suitable radiolabeled α_7 nAChR PET tracer would be important for 2 main reasons. First, the dose–response relationship in animals has been obscure (2,3), and because PET is becoming an increasingly important tool for demonstration of blood–brain barrier permeability and target occupancy, particularly in early dose-finding studies in humans (4,5), the availability of a α_7 nAChR PET radioligand to be used in humans would be needed for progressing novel drug candidates in clinical trials. Second, the levels of α_7 nAChR binding has been considered to be a predictor of neuronal functions and plasticity (6), and a α_7 nAChR PET radioligand would enable in vivo mapping and quantification of cerebral α_7 nAChR binding in different population or patient groups.

Several α_7 nAChR-selective PET radioligands have already been tested in animal and human studies (7–12). However, the α_7 nAChR has been a difficult target for PET radioligand development. In particular, none of the PET tracers developed so far have shown convincing blocking with α_7 nAChR-selective compounds that presumably do cross the blood–brain barrier and have pharmacologic effect on the α_7 nAChR. In conscious monkeys, with a semi-quantitative analysis the α_7 nAChR radioligand ¹¹C-CHIBA-1001 was not blocked to a significant extent by the structurally similar α_7 nAChR-selective partial agonist SSR180711 (9,13), and ¹¹C-(R)-MEQAA was blocked to an

Received Feb. 11, 2011; revision accepted Apr. 28, 2011.
For correspondence or reprints contact: Gitte Moos Knudsen, Neurobiology Research Unit, Rigshospitalet, Bldg. 9201, Blegdamsvej 9, DK-2100 Copenhagen, Denmark.
E-mail: gmk@nru.dk
Published online Aug. 9, 2011.
COPYRIGHT © 2011 by the Society of Nuclear Medicine, Inc.

equal extent with SSR180711 as well as the 5-HT₃ antagonist ondansetron, indicating lack of *in vivo* selectivity with this compound (10). Similarly, we previously validated ¹¹C-NS12857 as a PET tracer for the α₇nAChR; however, binding of this compound was also not blocked *in vivo* by either SSR180711 or the α₇nAChR functional antagonist NS6740 (8,14). Recently, the α₇nAChR PET radioligand ¹¹C-A-582941 was proposed to be displaceable by SSR180711 in a single conscious monkey (12), but no receptor occupancy was determined with this tracer. Accordingly, no measure of α₇nAChR occupancy by these compounds has previously been demonstrated with PET. Furthermore, because there are no suitable brain regions void of α₇nAChRs then no valid reference region exists (15). In the additional absence of completely blocked PET scans, or even valid partial α₇nAChR occupancy plotting, the non-specific binding of a PET radioligand, which is essential for evaluating the *in vivo* properties, cannot be evaluated.

Here we present the radiosynthesis and *in vivo* evaluation of 4-[5-[1-¹¹C-methyl-1*H*-pyrrol-2-yl]-1,3,4-oxadiazol-2-yl]-1,4-diazabicyclo[3.2.2]nonane (¹¹C-NS14492), a new selective orthosteric α₇nAChR agonist PET radioligand. We studied the *in vivo* biodistribution of ¹¹C-NS14492 in the pig brain and conducted blocking studies with pharmacologic doses of either NS14492 itself or with the structurally different α₇nAChR ligand SSR180711.

MATERIALS AND METHODS

Chemistry

The labeling precursor 4-[5-(1*H*-pyrrol-2-yl)-1,3,4-oxadiazol-2-yl]-1,4-diazabicyclo[3.2.2]nonane (desmethyl-NS14492) and the reference standard NS14492 were prepared at NeuroSearch A/S, Denmark. Solvents and reagents were purchased from Sigma-Aldrich and used without further purification.

Animal Procedures

Five female Danish Landrace pigs (mean weight ± SD, 19.0 ± 1.2 kg) were used in this study. After arrival, the animals were housed under standard conditions and were allowed to acclimatize for 1 wk before scanning. The animals were provided with straw bedding and environment enrichment, in the form of plastic balls and metal chains. On the scanning day, the pig was tranquilized by an intramuscular injection of 0.5 mg of midazolam per kilogram. Anesthesia was induced by intramuscular injection of a Zoletil veterinary mixture (tiletamine [1 mg/kg], zolazepam [1 mg/kg], xylazine [1 mg/kg], ketamine [1 mg/kg], metadon [0.15 mg/kg], and butorphanol [0.15 mg/kg]; Virbac Animal Health). After induction, anesthesia was maintained by intravenous infusion of propofol (10 mg/kg/h; B. Braun Melsugen). During anesthesia,

animals were endotracheally intubated and ventilated (volume, 250 mL; frequency, 15 per min). Venous access was granted through 2 venous lines in the peripheral milk veins, and an arterial line for blood sampling was inserted in the femoral artery after a minor incision. Vital signs, including blood pressure, temperature, and heart rate, were monitored throughout the duration of PET scanning. Immediately after scanning, the animals were sacrificed by intravenous injection of pentobarbital and lidocaine. All animal procedures were approved by the Danish Council for Animal Ethics (journal no. 2007/561-1320).

Radiochemical Synthesis of ¹¹C-NS14492

All irradiations were performed with the Scanditronix MC32 cyclotron at the PET and Cyclotron Unit at Copenhagen University Hospital, Rigshospitalet. ¹¹C-methane was produced in the ¹⁴N(p,α)¹¹C nuclear reaction by bombarding an aluminum gas target with a quartz insert containing a mixture of 90% nitrogen (AGA 6.0 nitrogen) and 10% hydrogen (AGA 5.0 hydrogen) gas (16). ¹¹C-methane was converted to ¹¹C-methyl iodide and ¹¹C-methyl trifluoromethanesulfonate (triflate) as previously described (17,18). ¹¹C-methyl triflate was transferred in a stream of helium to a 1.1-mL vial containing 0.3 mg of desmethyl-NS14492 fumarate dissolved in 300 μL of acetone and 10 μL of 1 M tetrabutylammonium hydroxide in methanol (Fig. 1). The resulting mixture was heated to 60°C for 3 min before purification by high-performance liquid chromatography (HPLC) with 0.1 v/v% phosphoric acid/ethanol 96% (90/10) at 6 mL/min. The product fraction (6 mL) was sterile-filtered during collection and diluted with 9 mL of 0.1 M phosphate buffer, pH 7. The HPLC system for purification of ¹¹C-NS14492 consisted of 2 Knauer pumps, an ultraviolet detector, an inline radioactivity detector, and a semipreparative reversed-phase C18 column (Luna C18(2), 5 μm, 10 × 250 mm; Phenomenex).

In Vitro Binding Assays

³H-cytisine (1.11 TBq/mmol) and ³H-α-bungarotoxin (2.22 TBq/mmol) were purchased from PerkinElmer Life and Analytic Sciences, respectively. (–)-Nicotine and *d*-tubocurarine were purchased from Sigma-Aldrich. All other chemicals were purchased from regular commercial sources and were of the purest grade available.

Tissue preparation and ³H-α-bungarotoxin binding were performed on rat cortical membranes as previously described (19). In brief, the assay was performed at 1 nM ³H-α-bungarotoxin (25 μL) in 50 mM tris-HCl buffer (pH 7.4) containing 120 mM NaCl, 5 mM KCl, 1 mM MgCl₂, 2.5 mM CaCl₂, and 0.01% bovine serum albumin in a final volume of 550 μL and incubated for 2 h at 37°C in triplicate. NS14492 (25 μL) was tested at final concentrations ranging from 0.1 to 100 nM. Nonspecific binding was determined in the presence of 1 mM (–)-nicotine. ³H-α-bungarotoxin binding to cellular membrane fractions from α₁β₁γδ nAChR-expressing TE671 cells was performed as earlier

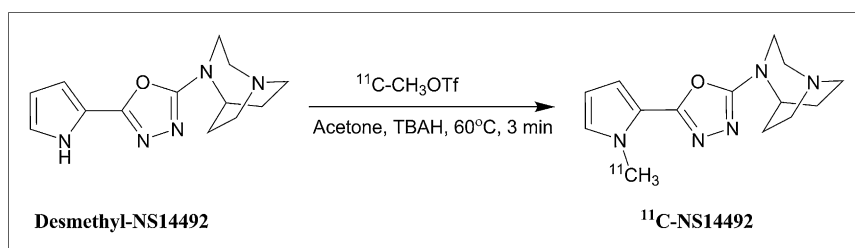


FIGURE 1. Radiochemical synthesis of ¹¹C-NS14492. OTf = triflate; TBAH = tetrabutylammonium hydroxide.

reported (20), and was, in brief, similar to the conditions used for ^3H - α -bungarotoxin binding to rat cortical membranes. Nonspecific binding was determined in the presence of 100 μM *d*-tubocurarine. NS14492 was tested at final concentrations ranging from 0.1 to 10 μM .

Preparation of tissue suspensions and ^3H -cytisine binding were performed on rat cortical membranes as previously described (21). In brief, the assay was performed at 1 nM ^3H -cytisine in 50 mM tris-HCl buffer (pH 7.4) and incubated for 90 min at 2°C in triplicate. NS14492 was tested at final concentrations ranging from 0.1 to 30 μM . Nonspecific binding was determined in the presence of 100 μM (-)-nicotine.

In all binding assays, incubations were terminated by rapid vacuum filtration. Filters used for termination of ^3H - α -bungarotoxin binding assays were presoaked in 0.1% polyethyleneimine, and filters were washed with ice-cold 50 mM Tris-HCl buffer containing 0.05% polyethyleneimine. Bound radioactivity on the filters was measured by conventional liquid scintillation counting, and dissociation constants of 0.90 nM for ^3H - α -bungarotoxin and 0.95 nM for ^3H -cytisine were used for calculation of affinity (K_i) values with the Cheng-Prusoff equation. Data are reported as mean \pm SEM ($n = 3$ –4 determinations).

PET Protocol

^{11}C -NS14492 was given as an intravenous bolus injection (injected dose, 499 ± 78 MBq; injected cold mass, 0.42 ± 0.65 μg , $n = 10$), and the pigs were subsequently scanned at baseline for 90 min in list mode with a high-resolution research tomography (HRRT) scanner (Siemens AG). Scanning was started at the time of injection (0 min). Immediately after the baseline scan (90 min), the $\alpha_7\text{nAChR}$ blocking agents were given intravenously (SSR180711, 1 or 10 mg/kg, or NS14492, 10 mg/kg, dissolved in saline), and the pigs were rescanned at either 30 min or 4 h later using the same PET protocol. During the first 15 min after injection, radioactivity in the whole blood was continuously measured using an ABSS autosampler (Allogg Technology) counting coincidences in a lead-shielded detector. Concurrently, arterial whole blood (10 mL) was sampled manually at 2.5, 5, 10, 20, 30, 50, 70, and 90 min after injection, and radioactivity in whole blood and plasma was measured using a well counter (Cobra 5003; Packard Instruments), which was cross-calibrated to the HRRT scanner and to the autosampler. Radiolabeled parent compound and metabolites were measured in plasma. The free fraction (f_p) of ^{11}C -NS14492 in pig plasma was measured using an equilibrium dialysis method as previously described (22) and calculated as the ratio between radioactivity in a buffer and plasma compartment after equilibrium between the chambers was reached.

Quantification of PET Data

Ninety-minute HRRT list-mode PET data were reconstructed using a standard iterative method as previously reported (23) (3-dimensional ordinary Poisson ordered-subset expectation maximization with point spread function, 10 iterations, and 16 subsets) into 38 dynamic frames of increasing length (6×10 , 6×20 , 4×30 , 9×60 , 2×180 , 8×300 , and 3×600 s). Images consisted of 207 planes of 256×256 voxels of $1.22 \times 1.22 \times 1.22$ mm. A summed image of all counts in the 90-min scan time for each pig was reconstructed and used for coregistration to a standardized MRI-based statistical atlas of the Danish Landrace pig brain, similar to that previously reported for the Göttingen minipig (24) using the program Register as previously described (22). Afterward, the

activity in volumes of interest, including the cerebellum, cortex (defined in the MRI-based atlas as the entire cortical gray matter), hippocampus, striatum, and thalamus, was extracted as radioactive concentrations (Bq/mL) in left and right hemispheres. Activity in striatum was averaged over the caudate nucleus and the putamen, whereas the thalamus was calculated as the average of activity in the medial and lateral thalamus. For the time-activity curves, standardized uptake values were calculated by normalizing radioactive concentration in volumes of interest (kBq/mL, average from left and right sides) to the injected dose corrected for animal weight (kBq/g), yielding the unit grams per milliliter.

Whole blood (10 mL) sampled during the PET scan was centrifuged at ambient temperature (1,500g, 7 min). The plasma was filtered through a 0.45- μm filter (13 or 25 mm polyvinylidene fluoride syringe filter; Whatman) before HPLC analysis with online radioactivity detection, as previously described (25). Because of the relatively fast metabolism of ^{11}C -NS14492, low parent compound fractions and noisy individual measurements were found at the late time points. Therefore, a population-based averaged metabolite curve of the 10 scans was constructed and subsequently used to correct plasma activity in the individual scans for parent compound fraction, thus obtaining the ^{11}C -NS14492 arterial input function for kinetic modeling. Regional ^{11}C -NS14492 distribution volumes (V_T) were calculated by a Logan graphical analysis with arterial input (26). Attempts were also made to quantify the ^{11}C -NS14492 PET data with compartment models. However, the 1-tissue-compartment model did not satisfactorily fit the data, and the 2-tissue-compartment model did not yield meaningful V_T values as the fitted k_4 rate constants approached zero. All kinetic modeling was done using PMOD software (version 3.0; PMOD Technologies Inc.). The occupancy of competing compound (NS14492 and SSR180711) was calculated by plotting V_T values in the baseline and blocked condition for 10 regions as previously described (27,28). In this plot, occupancy is calculated as the slope of the regression line, and the nondisplaceable distribution volume (V_{ND}) is determined by the intercept.

RESULTS

In Vitro Properties of NS14492

In rat cerebral cortical homogenates expressing both α_7 and $\alpha_4\beta_2^*$ nAChRs, binding assays for these receptors were done with the selective ligands ^3H - α -bungarotoxin and ^3H -cytisine, respectively. The affinity (K_i value) of NS14492 in displacement of $\alpha_7\text{nAChR}$ binding was 2.2 ± 0.8 nM, whereas for $\alpha_4\beta_2^*$ nAChRs it was 2.8 ± 1.1 μM . The affinity of NS14492 for $\alpha_1\beta_1\gamma\delta$ nAChR using ^3H - α -bungarotoxin binding to TE671 cell membranes was found to be greater than 10 μM .

NS14492 was also tested at 10 μM in a LeadProfilingScreen (Ricerca Biosciences) and using the National Institute of Mental Health's Psychoactive Drug Screening Program for binding to a broad range of 108 different receptors, transporters, and ion channels. The only targets for which greater than 50% inhibition was noted were the human 5-HT₃R (inhibition of ^3H -GR-65630 binding to recombinant receptors expressed in HEK-293 cells) and human $\alpha_3\beta_4^*$ nAChRs (inhibition of ^3H -epibatidine binding to human IMR-32 cells). In follow-up binding studies, NS14492 had a K_i of 0.17–0.28

μM for 5-HT₃R. The lipophilicity of NS14492 was calculated at a $\text{cLogD}_{7.4}$ of -0.96 using Pallas 2.1 (CompuDrug Inc.).

Radiochemistry

In a total synthesis time of 35 min, 400–1,700 MBq (860 ± 316 MBq, $n = 10$) of ¹¹C-NS14492 was produced on a fully automated system. The radiochemical purity was greater than 98%, with specific radioactivities at the time of injection in the range of 77–1,463 GBq/ μmol (795 ± 411 GBq/ μmol , $n = 10$). The radiochemical yield of ¹¹C-NS14492 production as measured from the preparative HPLC was 46%–68% ($56\% \pm 6\%$, $n = 11$).

PET

After intravenous injection, ¹¹C-NS14492 entered the pig brain and showed high brain uptake (Fig. 2; peak standardized uptake value, ~ 2.2). The highest binding of ¹¹C-NS14492 was found in the thalamus and cortical areas, moderate binding was seen in the striatum, and relatively low binding was observed in the cerebellum. The rapid decline in the tissue activity curves after peak uptake indicates reversible binding of ¹¹C-NS14492 within the 90-min scanning time applied in this study. The regional distribution of ¹¹C-NS14492 in the pig brain is shown in Figure 3.

Regional ¹¹C-NS14492 V_T values are shown in Figure 4; the largest values were found in the cortex, hippocampus, and thalamic areas, and they were on the order of 8–9 mL/ cm^3 . Pretreatment with NS14492 and pretreatment with SSR180711 both led to a decrease in V_T in all regions, including the cerebellum (Fig. 4). Pretreatment with 1 mg of SSR180711 per kilogram resulted in 61% occupancy, whereas 10 mg of SSR180711 per kilogram resulted in 69% and 81% occupancy in 2 different pigs (Table 1),

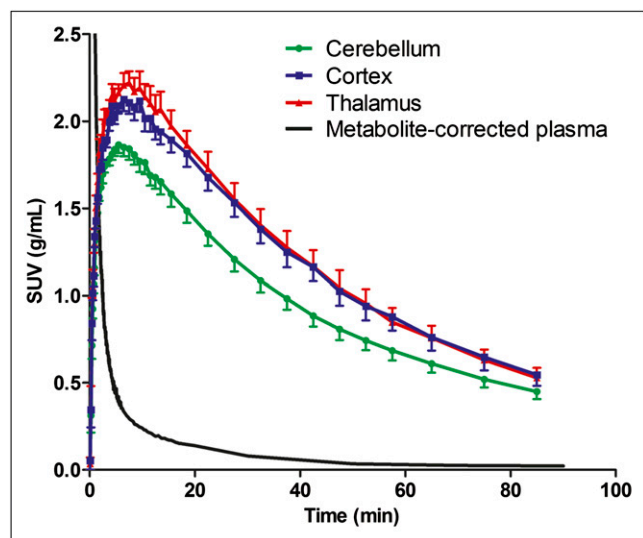


FIGURE 2. Regional time-activity curves of ¹¹C-NS14492 in pig brain at baseline ($n = 5$). Mean standardized uptake values computed as radioactivity concentration normalized to injected dose per body weight are shown for cortex, thalamus, cerebellum, and average radiolabeled parent compound concentration. Error bars indicate SEM. SUV = standardized uptake value.

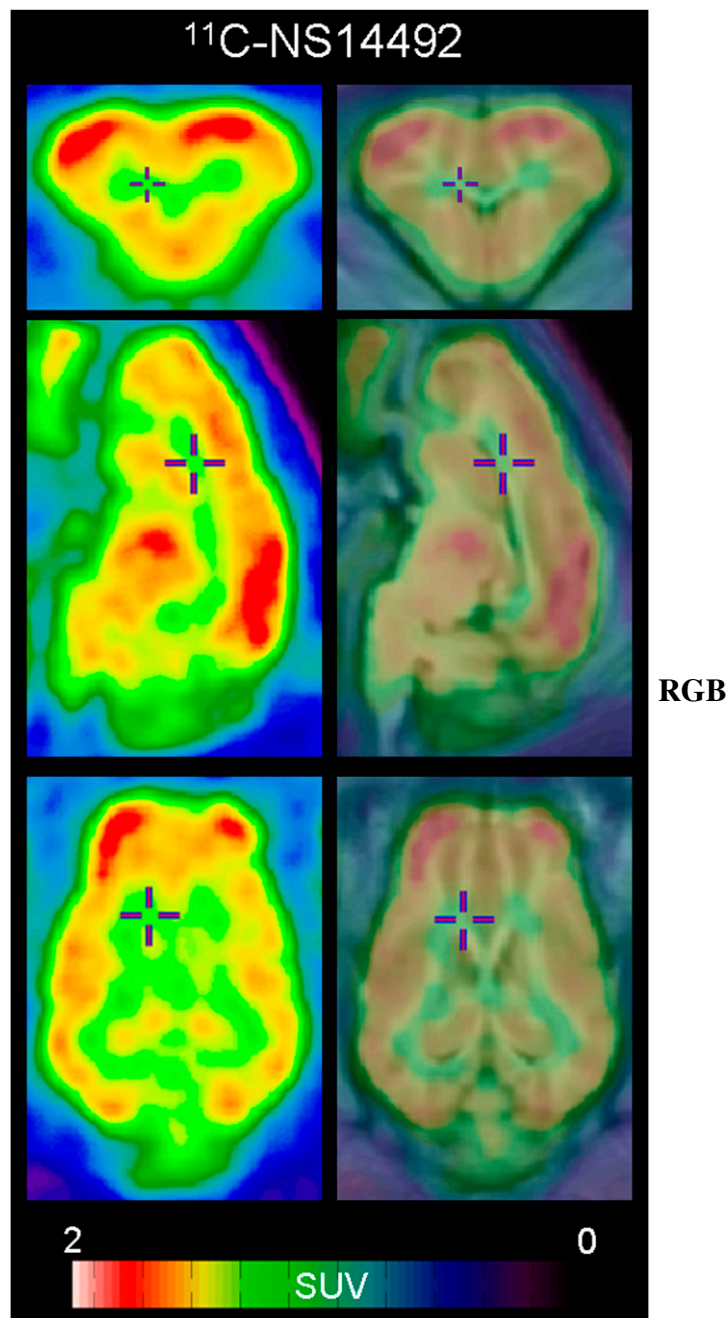


FIGURE 3. Representative coronal (top), sagittal (middle), and horizontal (bottom) PET images summed from 0- to 90-min scanning showing distribution of ¹¹C-NS14492 in pig brain. Left column shows PET images filtered using $3 \times 3 \times 3$ mm gaussian filter. Right column, same PET images coregistered and overlaid on standard pig brain.

suggesting a dose-dependent receptor occupancy. Also, increasing the time interval between pretreatment with 10 mg of NS14492 per kilogram and the start of scanning from 30 min to 4 h decreased receptor occupancy from 75% to 60%. In the pig scanned at 4 h after administration of 10 mg of NS14492 per kilogram, the NS14492 plasma concentration was measured with HPLC at 842 and 80 ng/mL,

RGB

RGB

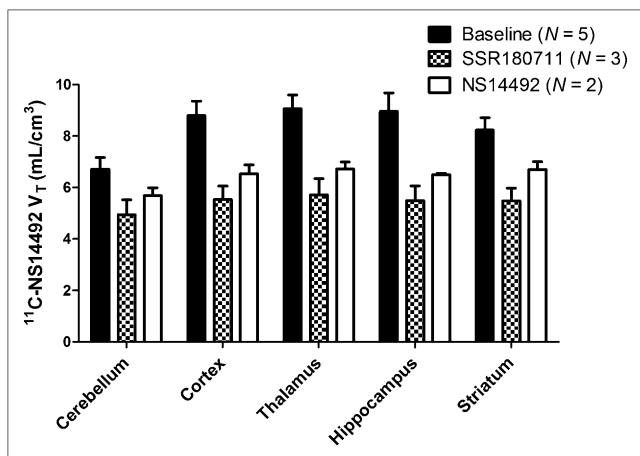


FIGURE 4. Regional invasive Logan plot V_T s of ^{11}C -NS14492 in pig brain are shown at baseline and after $\alpha_7\text{nAChR}$ blockade with SSR180711 (1 or 10 mg/kg administered 30 min before second scan) or NS14492 (10 mg/kg administered 30 min or 4 h before second scan). Bars indicate mean \pm SEM.

30 min and 4 h after intravenous injection, respectively. On the basis of the occupancy plots from the individual animals (Fig. 5), V_{ND} of ^{11}C -NS14492 was on average 4.75 ± 1.16 mL/cm^3 (mean \pm SD, $n = 5$), meaning that the specific V_{TS} were on the order of almost 5 mL/cm^3 (Table 1). In all the animals, the slope of the occupancy plot linear regression line was significantly different from zero (Fig. 5).

After intravenous injection, the parent fraction of ^{11}C -NS14492 declined rapidly (Fig. 6); 10% of the total plasma radioactivity attributable to parent compound remained after 50 min. No radiolabeled lipophilic metabolites of ^{11}C -NS14492 were detected in the pig plasma, as indicated by lack of distinct peaks in the lipophilic range on the radiochromatograms (data not shown). The free fraction of ^{11}C -NS14492 in pig plasma was on average $67.2\% \pm 4.7\%$ (mean \pm SD, $n = 5$).

DISCUSSION

Here, we present the radiosynthesis and in vivo evaluation of a novel $\alpha_7\text{nAChR}$ PET radioligand, ^{11}C -NS14492, showing high blood–brain barrier passage, in accordance with the observed high fraction of non–protein-bound ^{11}C -NS14492. The biodistribution of ^{11}C -NS14492 in the pig brain was in accordance with the distribution of

$\alpha_7\text{nAChR}$ binding sites in the human brain in vitro as measured with ^{125}I - α -bungarotoxin autoradiography (15). Furthermore, the in vitro autoradiographic distribution of ^{11}C -NS14492 in the pig brain was in accordance with that of ^{125}I - α -bungarotoxin (Supplemental Fig. 1; supplemental materials are available online only at <http://jnm.snmjournals.org>). Pretreatment with unlabeled NS14492 or by the structurally different $\alpha_7\text{nAChR}$ ligand SSR180711 consistently reduced ^{11}C -NS14492 binding in the pig brain, supporting the finding that the radioligand binds specifically to $\alpha_7\text{nAChR}$ also in vivo. ^{11}C -NS14492 is thus the first PET radioligand that convincingly has been able to determine $\alpha_7\text{nAChR}$ occupancy levels in vivo, providing compelling evidence that ^{11}C -NS14492 is a good candidate PET radioligand for future studies of $\alpha_7\text{nAChR}$ binding also in humans.

The in vitro characterization revealed that NS14492 is a high-affinity and selective $\alpha_7\text{nAChR}$ ligand with little or no affinity to other nicotinic receptor subtypes. With a K_i of 2.2 nM against $\alpha_7\text{nAChR}$, NS14492 thus compares favorably to some previously used PET radioligands displaying lower affinity for $\alpha_7\text{nAChR}$ (10,12,29). Because the specific binding signal is proportional to the affinity of the radioligand for its target, an optimal $\alpha_7\text{nAChR}$ PET radioligand probably will require a relatively high affinity. For NS14492, the average selectivity for $\alpha_7\text{nAChR}$ over 5-HT₃R was approximately 100-fold, based on K_i values for $\alpha_7\text{nAChR}$ and 5-HT₃R. This selectivity is of particular importance because many $\alpha_7\text{nAChR}$ ligands display cross-selectivity to the structurally similar 5-HT₃R. Other $\alpha_7\text{nAChR}$ PET radioligands were much less selective for $\alpha_7\text{nAChR}$ over 5-HT₃R (~3-fold), and equal displacement in vivo by pretreatments blocking either of the receptors was found (10). Also, when compared with the $\alpha_4\beta_2^*$ and $\alpha_1\beta_1\gamma\delta$ nAChRs, NS14492 was highly selective for $\alpha_7\text{nAChR}$ (>1,000-fold).

The in vitro characterization corresponded well to the outcome of the PET scans; systemic pretreatment with NS14492 or SSR180711 decreased V_T , supporting the in vivo selectivity of ^{11}C -NS14492 binding for $\alpha_7\text{nAChR}$. The decreases in ^{11}C -NS14492 V_T were found across all regions examined, including the cerebellum. This means—as expected—that the cerebellum is not appropriate as a reference region for $\alpha_7\text{nAChR}$ quantification. In humans, the larger brain size may enable use of other reference regions that are not quantifiable in the pig brain. For example, a

TABLE 1
 $\alpha_7\text{nAChR}$ Occupancy in Pig Brain Quantified with ^{11}C -NS14492 V_T

Pig no.	Pretreatment	Interscan interval	Drug occupancy (%)	V_{ND} (mL/cm^3)	Specific cortical V_T (baseline $V_{T^{\text{cortex}}} - V_{\text{ND}}$)
1	NS14492, 10 mg/kg	30 min	75	5.84	3.99
2	NS14492, 10 mg/kg	4 h	60	5.13	3.09
3	SSR180711, 10 mg/kg	30 min	81	5.73	4.63
4	SSR180711, 10 mg/kg	30 min	69	3.68	3.77
5	SSR180711, 1 mg/kg	30 min	61	3.37	4.79

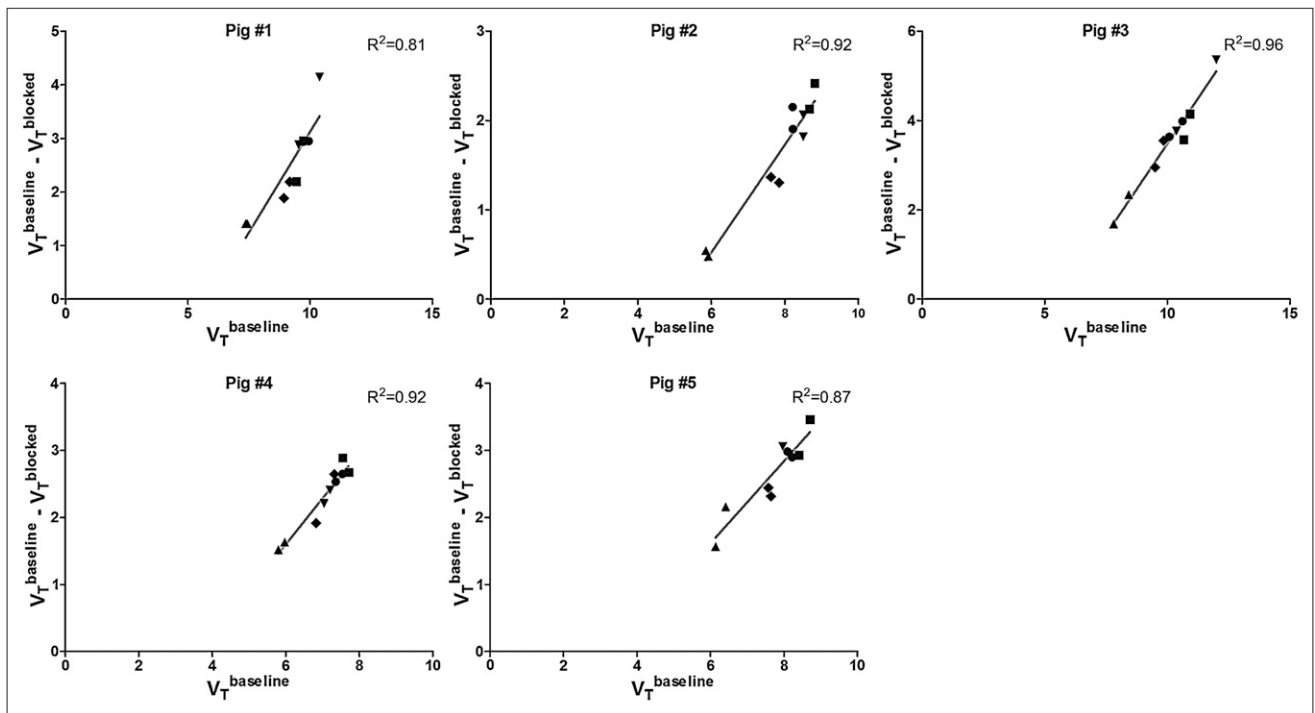


FIGURE 5. Occupancy plots of ^{11}C -NS14492 V_T s at baseline and in blocked scan for each of 5 pigs. Fraction of $\alpha_7\text{nAChR}$ occupancy by blocking agent (NS14492 or SSR180711) is measured as slope of regression line, and ^{11}C -NS14492 V_{ND} is intercept at y-axis. R^2 values are shown for each plot. • = cortex; ■ = thalamus; ▲ = cerebellum; ▼ = hippocampus; ◆ = striatum.

large white matter region, such as the corpus callosum, which has been used as a reference region for quantification of PET data from nicotinic $\alpha_4\beta_2^*$ (30), could possibly serve as a reference region in $\alpha_7\text{nAChR}$ PET quantification in humans. However, this region was not defined in the available pig space atlas, and even if it was, it would most likely be too small to be accurately measured. In the absence of an appropriate reference region, we determined the nondisplaceable binding from the occupancy plot.

In blocking studies, we found signs of a dose–occupancy relationship in that pretreatment with 10 mg of SSR180711 per kilogram led to an average $\alpha_7\text{nAChR}$ occupancy of 75%, and 1 mg of SSR180711 per kilogram resulted in 61% receptor occupancy. Pretreatment with NS14492 (10 mg/kg) 30 min before the blocked PET scan led to $\alpha_7\text{nAChR}$ occupancy of 75%, and increasing the interscan interval to 4 h decreased the receptor occupancy to 60%, presumably because of the lower NS14492 plasma levels found after 4 h, compared with 30 min, after intravenous injection. However, we cannot exclude that the longer interval between the baseline and blocked scans could play a role. Taken together, these results suggest that ^{11}C -NS14492 binding is blocked dose-dependently, supporting its use for the *in vivo* assessment of $\alpha_7\text{nAChR}$ occupancy in the living brain. Such a utility would be relevant for dose-finding studies in clinical drug development. ^{11}C -NS14492 is thus the first $\alpha_7\text{nAChR}$ PET radioligand that shows promise for measuring $\alpha_7\text{nAChR}$ occupancy.

The average nonspecific binding in the pig brain, V_{ND} , of ^{11}C -NS14492 as determined by the occupancy plot was 4.75 mL/cm³ and thus comprised approximately 50% of the V_T in the high-binding regions. This ratio of specific-to-nonspecific binding is comparable to that obtained with other PET tracers used in the human brain (22,30,31). The previously validated $\alpha_7\text{nAChR}$ PET radioligand ^{11}C -CHIBA-1001

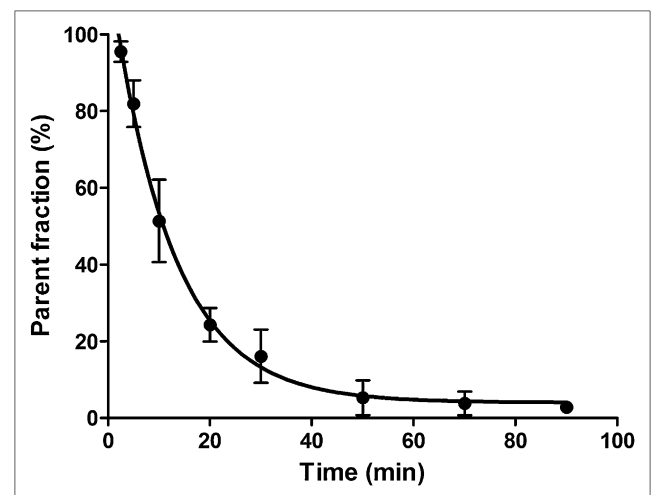


FIGURE 6. Relative radioactive parent compound in pig plasma as function of time after intravenous injection of ^{11}C -NS14492. Average of measurements from 5 baseline PET scans is shown. Error bars represent SD. Solid line constitutes single exponential decay function fitted to data.

was not convincingly blocked by the structurally similar compound SSR180711, probably because of high nonspecific binding in vivo (9,11) and ³H-CHIBA-1001 was not displaced by α -bungarotoxin, most likely because of nontarget binding that was too high (29). In the absence of valid data for the nonspecific binding of any of the previously published α ₇nAChR PET radioligands, a numeric comparison to the in vivo V_{ND} of ¹¹C-NS14492 is not possible.

The systemic metabolism of ¹¹C-NS14492 in pigs after intravenous injection was relatively fast, and 20 min after intravenous injection, about 20% of the total plasma radioactivity arose from the parent compound. Ninety minutes after intravenous injection, less than 2% of total radioactivity represented the parent compound, and no indication of changed metabolism by pharmacologic blockade of the α ₇nAChR was observed. The fast metabolism of ¹¹C-NS14492 makes it difficult to reliably determine the parent compound fraction at the late time points, complicating the use of the metabolite data from the individual pigs and prompting us to use a population-based metabolite correction. No lipophilic metabolites that potentially could cross the blood–brain barrier and disturb the binding signal were observed in the radiochromatograms of pig plasma after intravenous injection of ¹¹C-NS14492. This finding is in accordance with metabolism of ¹¹C-NS14492 occurring by demethylation at the labeled nitrogen substituent. Thus, we expect that the *N*-oxide would be the main metabolite, but further studies are needed to establish the exact metabolic route of ¹¹C-NS14492.

CONCLUSION

¹¹C-NS14492 is a promising PET radioligand for mapping and quantifying α ₇nAChR in the living brain showing high uptake in the appropriate regions. Furthermore, ¹¹C-NS14492 is blocked by the structurally different α ₇nAChR ligand SSR180711 and unlabeled NS14492, suggesting that it can be used to measure α ₇nAChR occupancy in vivo.

DISCLOSURE STATEMENT

The costs of publication of this article were defrayed in part by the payment of page charges. Therefore, and solely to indicate this fact, this article is hereby marked “advertisement” in accordance with 18 USC section 1734.

ACKNOWLEDGMENTS

We acknowledge the technical assistance of Hans Jørgen Jensen, Bente Dall, Jonni Heberg, Mette Værum Olesen, and Letty Klarskov. This study was partially supported by the Lundbeck Foundation and Faculty of Health Sciences, University of Copenhagen, Danish Ministry of Science, Technology and Innovation (grant 08-034107) and EU framework program DiMI (LSHB-CT-2005-512146). K_i determinations at neuroreceptors were generously provided by the National Institute of Mental Health’s Psychoactive

Drug Screening Program (contract HHSN-271-2008-00025-C; NIMH PDSP). The NIMH PDSP is directed by Bryan L. Roth at the University of North Carolina at Chapel Hill and Project Officer Jamie Driscoll at NIMH, Bethesda. For experimental details, refer to the PDSP Website, <http://pdsp.med.unc.edu/>. No other potential conflict of interest relevant to this article was reported.

REFERENCES

1. Freedman R, Olincy A, Buchanan RW, et al. Initial phase 2 trial of a nicotinic agonist in schizophrenia. *Am J Psychiatry*. 2008;165:1040–1047.
2. Thomsen MS, Hansen HH, Timmerman DB, Mikkelsen JD. Cognitive improvement by activation of alpha7 nicotinic acetylcholine receptors: from animal models to human pathophysiology. *Curr Pharm Des*. 2010;16:323–343.
3. Pichat P, Bergis OE, Terranova JP, et al. SSR180711, a novel selective alpha7 nicotinic receptor partial agonist: (II) efficacy in experimental models predictive of activity against cognitive symptoms of schizophrenia. *Neuropsychopharmacology*. 2007;32:17–34.
4. Gee AD. Neuropharmacology and drug development. *Br Med Bull*. 2003;65:169–177.
5. Lee CM, Farde L. Using positron emission tomography to facilitate CNS drug development. *Trends Pharmacol Sci*. 2006;27:310–316.
6. Christensen DZ, Mikkelsen JD, Hansen HH, Thomsen MS. Repeated administration of alpha7 nicotinic acetylcholine receptor (nAChR) agonists, but not positive allosteric modulators, increases alpha7 nAChR levels in the brain. *J Neurochem*. 2010;114:1205–1216.
7. Deuther-Conrad W, Fischer S, Hiller A, et al. Molecular imaging of alpha7 nicotinic acetylcholine receptors: design and evaluation of the potent radioligand [¹⁸F]NS10743. *Eur J Nucl Med Mol Imaging*. 2009;36:791–800.
8. Ettrup A, Mikkelsen JD, Marcussen AB, et al. [¹¹C]NS12857 is a novel PET ligand for imaging α ₇-nicotinic receptors: preliminary data from the pig brain. In: *2009 Neuroscience Meeting Planner*. Chicago, IL: Society for Neuroscience; 2009. Available at: <http://www.abstractsonline.com/Plan/ViewAbstract.aspx?sKey=f59161a9-524e-490a-a210-de273ae6e9eb&cKey=2b78a2e6-4dce-48b5-8d66-7d81b35749f9&mKey=%7b081f7976-E4CD-4F3D-A0AF-E8387992A658%7d>. Accessed July 21, 2011.
9. Hashimoto K, Nishiyama S, Ohba H, et al. [¹¹C]CHIBA-1001 as a novel PET ligand for alpha7 nicotinic receptors in the brain: a PET study in conscious monkeys. *PLoS ONE*. 2008;3:e3231.
10. Ogawa M, Nishiyama S, Tsukada H, et al. Synthesis and evaluation of new imaging agent for central nicotinic acetylcholine receptor alpha7 subtype. *Nucl Med Biol*. 2010;37:347–355.
11. Toyohara J, Sakata M, Wu J, et al. Preclinical and the first clinical studies on [¹¹C]CHIBA-1001 for mapping alpha7 nicotinic receptors by positron emission tomography. *Ann Nucl Med*. 2009;23:301–309.
12. Toyohara J, Ishiwata K, Sakata M, et al. In vivo evaluation of alpha7 nicotinic acetylcholine receptor agonists [¹¹C]A-582941 and [¹¹C]A-844606 in mice and conscious monkeys. *PLoS ONE*. 2010;5:e8961.
13. Biton B, Bergis OE, Galli F, et al. SSR180711, a novel selective alpha7 nicotinic receptor partial agonist: (1) binding and functional profile. *Neuropsychopharmacology*. 2007;32:1–16.
14. Briggs CA, Gronlien JH, Curzon P, et al. Role of channel activation in cognitive enhancement mediated by alpha7 nicotinic acetylcholine receptors. *Br J Pharmacol*. 2009;158:1486–1494.
15. Breese CR, Adams C, Logel J, et al. Comparison of the regional expression of nicotinic acetylcholine receptor alpha7 mRNA and [¹²⁵I]-alpha-bungarotoxin binding in human postmortem brain. *J Comp Neurol*. 1997;387:385–398.
16. Kozirowski J, Larsen P, Gillings N. A quartz-lined carbon-11 target: striving for increased yield and specific activity. *Nucl Med Biol*. 2010;37:943–948.
17. Jewett DM. A simple synthesis of [¹¹C]methyl triflate. *Int J Rad Appl Instrum [A]*. 1992;43:1383–1385.
18. Larsen P, Ulin J, Dahlstrom K, Jensen M. Synthesis of [¹¹C]iodomethane by iodination of [¹¹C]methane. *Appl Radiat Isot*. 1997;48:153–157.
19. Andreasen JT, Andersen KK, Nielsen EO, Mathiasen L, Mirza NR. Nicotine and clozapine selectively reverse a PCP-induced deficit of PPI in BALB/cByJ but not NMRI mice: comparison with risperidone. *Behav Brain Res*. 2006;167:118–127.
20. Lukas RJ. Interactions of anti-nicotinic acetylcholine receptor antibodies at alpha-bungarotoxin binding sites across species and tissues. *Brain Res*. 1986;387:119–125.

21. Nielsen SF, Nielsen EO, Olsen GM, Liljefors T, Peters D. Novel potent ligands for the central nicotinic acetylcholine receptor: synthesis, receptor binding, and 3D-QSAR analysis. *J Med Chem.* 2000;43:2217–2226.
22. Kornum BR, Lind NM, Gillings N, Marner L, Andersen F, Knudsen GM. Evaluation of the novel 5-HT₄ receptor PET ligand [¹¹C]SB207145 in the Gottingen minipig. *J Cereb Blood Flow Metab.* 2009;29:186–196.
23. Sureau FC, Reader AJ, Comtat C, et al. Impact of image-space resolution modeling for studies with the high-resolution research tomograph. *J Nucl Med.* 2008;49:1000–1008.
24. Watanabe H, Andersen F, Simonsen CZ, Evans SM, Gjedde A, Cumming P. MR-based statistical atlas of the Gottingen minipig brain. *Neuroimage.* 2001;14:1089–1096.
25. Gillings N. A restricted access material for rapid analysis of [¹¹C]-labeled radiopharmaceuticals and their metabolites in plasma. *Nucl Med Biol.* 2009;36:961–965.
26. Logan J, Fowler JS, Volkow ND, et al. Graphical analysis of reversible radioligand binding from time-activity measurements applied to [N-¹¹C-methyl]-(-)-cocaine PET studies in human subjects. *J Cereb Blood Flow Metab.* 1990;10:740–747.
27. Cunningham VJ, Rabiner EA, Slifstein M, Laruelle M, Gunn RN. Measuring drug occupancy in the absence of a reference region: the Lassen plot re-visited. *J Cereb Blood Flow Metab.* 2010;30:46–50.
28. Pinborg LH, Videbaek C, Ziebell M, et al. [¹²³I]epidepride binding to cerebellar dopamine D₂/D₃ receptors is displaceable: implications for the use of cerebellum as a reference region. *Neuroimage.* 2007;34:1450–1453.
29. Tanibuchi Y, Wu J, Toyohara J, Fujita Y, Iyo M, Hashimoto K. Characterization of [³H]CHIBA-1001 binding to alpha7 nicotinic acetylcholine receptors in the brain from rat, monkey, and human. *Brain Res.* 2010;1348:200–208.
30. Kendziorra K, Wolf H, Meyer PM, et al. Decreased cerebral alpha4beta2* nicotinic acetylcholine receptor availability in patients with mild cognitive impairment and Alzheimer's disease assessed with positron emission tomography. *Eur J Nucl Med Mol Imaging.* 2011;38:515–525.
31. Pinborg LH, Adams KH, Svarer C, et al. Quantification of 5-HT_{2A} receptors in the human brain using [¹⁸F]altanserin-PET and the bolus/infusion approach. *J Cereb Blood Flow Metab.* 2003;23:985–996.